

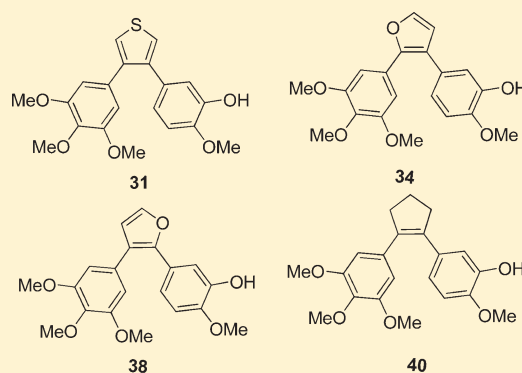
Regioselective Suzuki Coupling of Dihaloheteroaromatic Compounds as a Rapid Strategy To Synthesize Potent Rigid Combretastatin Analogues

Sewan Theeramunkong,[†] Antonio Caldarelli,[†] Alberto Massarotti, Silvio Aprile, Diego Caprioglio, Roberta Zaninetti, Alessia Teruggi, Tracey Pirali, Giorgio Grosa, Gian Cesare Tron,* and Armando A. Genazzani

Dipartimento di Scienze Chimiche, Alimentari, Farmaceutiche e Farmacologiche, Università degli Studi del Piemonte Orientale "A. Avogadro", Via Bovio 6, 28100 Novara, Italy

Supporting Information

ABSTRACT: Combretastatin A-4 (CA-4) is a potent tubulin depolymerizing agent able to inhibit tumor growth and with antivascular effects. Although it is in clinical trials, the search for novel analogues that may display better/different features is still ongoing. In this manuscript we describe the synthesis of novel constrained analogues of CA-4 obtained in only two synthetic steps exploiting a regioselective Suzuki coupling of dihalogenated heteroaromatic and alicyclic compounds. All the compounds synthesized have been evaluated for cytotoxicity and for their ability to inhibit tubulin assembly. One of them, **38**, displayed low nanomolar cytotoxicity and proved to have a pharmacodynamic profile similar to that of CA-4 and a better pharmacokinetic profile, but most important of all, this synthetic strategy may pave the way for the easy and rapid generation of novel rigid analogues of combretastatins.



INTRODUCTION

Combretastatin A-4 (CA-4, **1**) is a natural product derived from the African bush willow *Combretum caffrum* and has been first described over 20 years ago.¹ It is a strong tubulin depolymerizing agent and therefore inhibits tumor growth and has antivascular effects.² Its prodrug (disodium salt water-soluble phosphate derivative) has now entered clinical trials for both solid and liquid tumors.³ Similarly, a close derivative of combretastatin A4 (AVE8062)⁴ is also undergoing clinical trials. A number of trials have been initiated with these drugs (www.clinicaltrials.gov), and both compounds have demonstrated a sufficient safety profile in phase I trials, suggesting that this may be a viable therapeutic strategy.

Despite its low molecular weight and simple molecular structure, CA-4 (Figure 1) is one of the most powerful inhibitors of tubulin polymerization known to date. The structure can be divided into three separate components, the two rings (usually termed A and B) and the olefinic bridge. The structure–activity relationship (SAR) of CA-4 has been investigated thoroughly by a number of groups and is reasonably well-understood,⁵ although full SAR comprehension may be in part hampered by synthetic limitations and by literature bias. In brief, it is thought that the cis-configuration of the olefinic bridge, the presence of the 3,4,5-trimethoxy group on ring A, and the para-methoxy group on ring B are all fundamental for antitubulin activity. Nonetheless, active compounds not obeying this general rule have been described.⁶

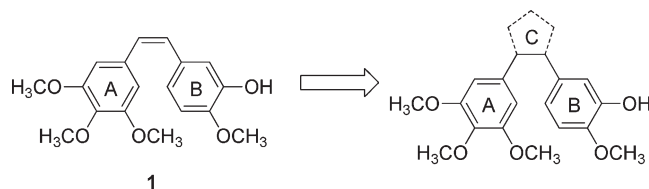


Figure 1. Rationale for the constraint of combretastatin A-4.

It is important to note that (i) the cis olefinic bridge is able to undergo rapid cis–trans isomerization under the influence of heat, light, and protic media⁵ and that (ii) the olefinic bridge represents a weak point for metabolic stability.⁷ It is therefore not surprising that a number of studies have attempted to replace the olefinic bridge, in particular with more rigid and metabolically stable structures able to maintain the correct conformation of the two adjacent rings.^{5,8} To this end, one of the strategies consists of the replacement of the olefinic bond with five-membered heterocyclic rings (Figure 1). Many of these novel compounds have been shown to be active, and indeed, some of the new compounds have been shown to display an increased potency. A second reason to replace the olefinic bridge is given by the difficulty in adding moieties to the two ring

Received: January 26, 2011

Published: June 22, 2011

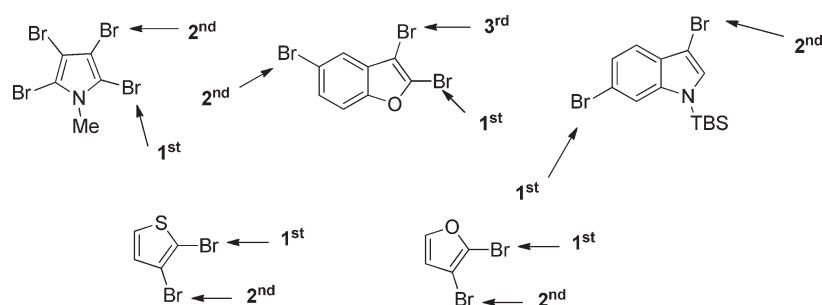
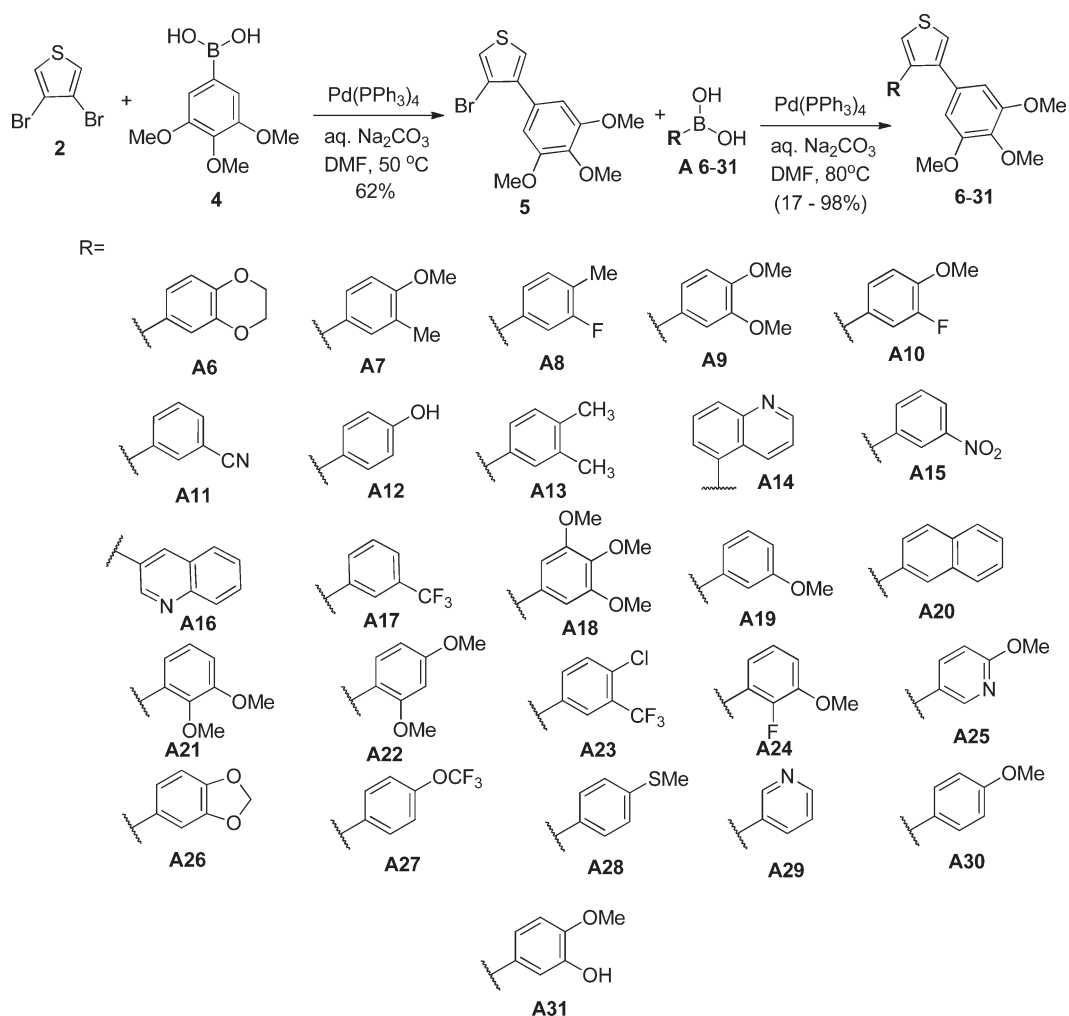


Figure 2. Selected examples of regioselective couplings of polyhaloheteroaromatic compounds.

Scheme 1. Synthesis of Combretathiophenes 6–31



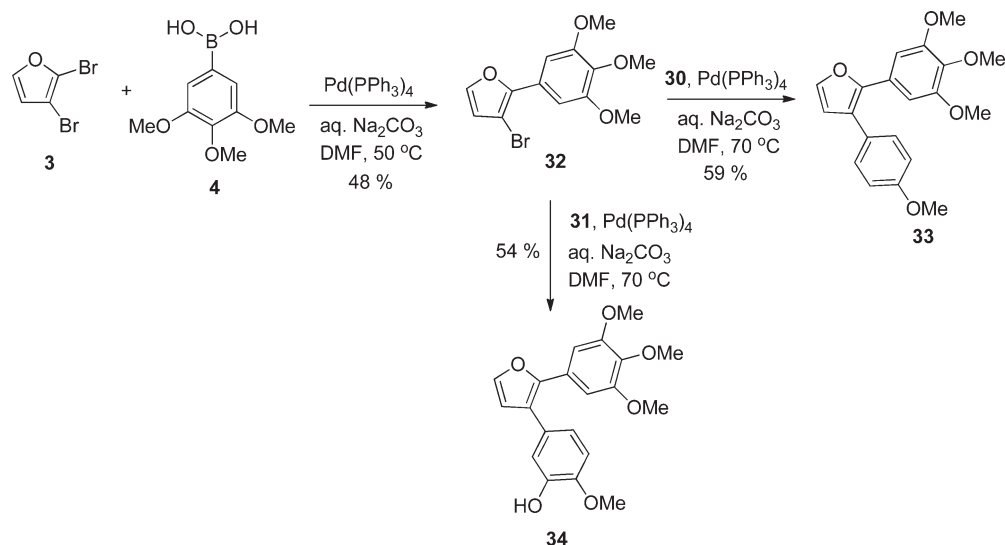
structures, as both appear to have direct interactions with tubulin. For example, to generate dual-acting drugs or drugs that bear additional functionalities, it may be envisaged that a ring replacing the olefinic ring may be the best harbor. Indeed, this has been shown to be possible.⁹

Although exceptions are well documented,¹⁰ one possible concern regarding this strategy is due to an increase of the number of synthetic steps required (compared to the synthesis of CA-4)¹¹ which can hamper a full exploitation of SAR studies. Second, it is difficult to unravel how modifications in the olefinic bridge

impact changes on the two rings, as it is difficult to compare data from different laboratories and different rigidified series.

Following this line of thought, we were intrigued by the possibility of generating heterocyclic analogues of combretastatin through a regioselective Suzuki coupling of polyhalogenated heteroaromatics. In the past decade this strategy has gained a prominent role in the synthesis of pharmaceuticals and natural products thanks to the possibility of discriminating between the reactivities of the carbon–halogen bonds in the oxidative addition step (Figure 2).¹²

Scheme 2. Synthesis of Combretafurans 33 and 34



Indeed, this strategy would enable us to generate, also through parallel synthesis with a minimum number of synthetic steps, a series of rigidified CA-4 analogues bearing a number of substituents. If this strategy were to work, it would be possible to evaluate methodically an increased number of ring A and B substitutions to generate a complete SAR of CA-4. The limit on the number of analogues generated would be only given by the number of polyhalogenated heteroaromatics available or synthesizable.

In this manuscript, we describe the synthesis and the biological evaluation of new furan, thiophene, and cyclopentene rigid analogues of CA-4 prepared in only two synthetic steps using a regioselective Suzuki coupling strategy. Following this strategy, we now report two rigidified analogues that display IC_{50} for cytotoxicity in the low nanomolar range and, more importantly, a strategy to develop limitless CA-4 analogues in few synthetic steps.

CHEMISTRY

To accomplish our task, we decided to use both symmetrical and nonsymmetrical dihalogenated heterocyclic rings, namely, the commercially available 3,4-dibromothiophene (**2**) and the 2,3-dibromofuran (**3**).

Starting with **2**, we decided to insert the 3,4,5-trimethoxyphenyl group in the first step, as this moiety can behave as an anchor in the tubulin binding site and to examine several substitutions on the other side that correspond to the B-ring of CA-4. Several experimental conditions were tested in order to reduce the amount of the symmetrical disubstituted analogue obtainable during the first step. Under these optimized conditions (3:1 thiophene/boronic acid, sodium carbonate, DMF, 50 °C) we were able to obtain the intermediate **5** in 62% yield and to recover the unreacted dibromothiophene without observing the formation of the bis-adduct. With this intermediate in our hands, we selected a library of boronic acid derivatives (**A6–A31**) bearing different substituents and coupled them to **5** to give a library of 25 combretathiophenes (**6–31**) (Scheme 1).

The experience in the combretastatin field suggests that the presence of a hydroxy group in the meta position is crucial. Yet the presence of this moiety, which confers potency to CA-4 and

to its analogues, usually leads to an increased number of synthetic steps, with the use of protecting groups. It is important to stress that the Suzuki reaction does not require the protection of the $-OH$ group, which confers potency to CA-4, being involved in a key hydrogen-bond interaction with tubulin.¹³ Indeed, the experience in the combretastatin field suggests that the presence of a phenolic group in the meta position imparts an increased number of synthetic steps, a more complicated synthetic plan and a reduced overall yield.¹⁴

For the synthesis of combretafurans starting from **3**, we capitalized on the different reactivity in the oxidative coupling step between the two carbon–bromine bonds. In this way, it was possible to insert the first substituted phenyl ring at the 2-position (3,4,5-trimethoxyphenyl, 4-methoxyphenyl, and 3-hydroxy-4-methoxyphenyl) to give **32**, **35**, and **37**, respectively. Also in this case, we did not observe the formation of bis-adduct byproducts.

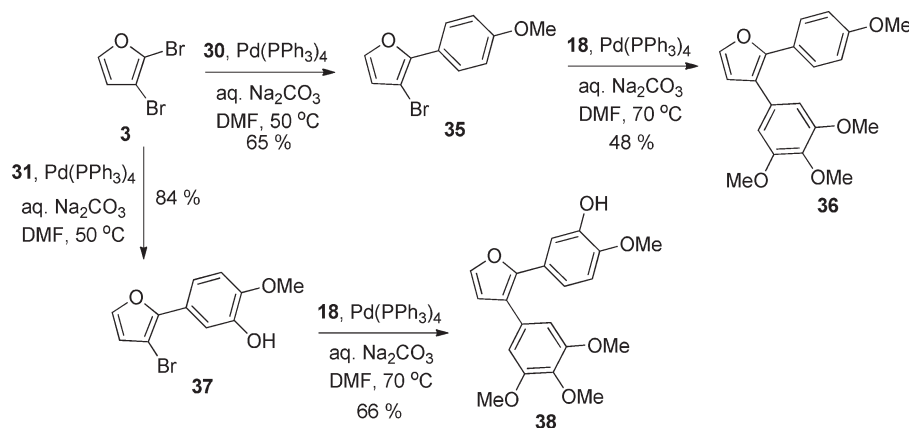
These intermediates were then coupled with the appropriate boronic acid (**18**, **30**, **31**) to give the final combretafurans **33**, **34**, **36**, and **38** (Schemes 2 and 3).

Finally, in order to demonstrate the generality of this concept, we prepared the true rigid analogue of combretastatin, replacing the olefinic double bond with a cyclopentene. Starting with the commercially available 1,2-dibromocyclopent-1-ene and using our same reaction conditions for the symmetrical dihaloheteroaromatics, we obtained the monosubstituted analogue **39** in 23% yield. This low yield was probably due to the thermal instability of the dibromo analogue and not to the formation of the bis-adduct byproduct. Compound **39** was then coupled with (3-hydroxy-4-methoxyphenyl)boronic acid (**31**) to give the final compound **40** in 44% yield (Scheme 4).

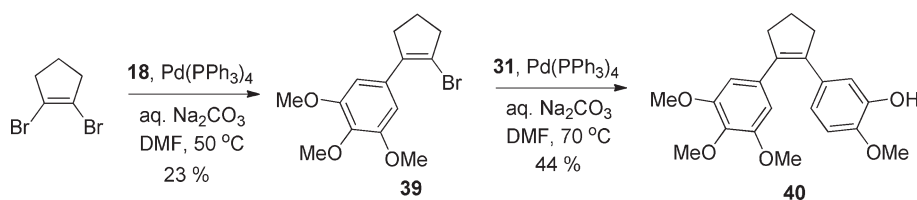
BIOLOGICAL RESULTS

To evaluate the cytotoxic nature of the synthesized compounds, we used a neuroblastoma cell line (SH-SY5Y) that we had previously characterized as sensitive to combretastatin A-4.¹⁵ As an initial screening, we incubated all compounds at 1 μM , as we aimed at identifying only compounds with nanomolar potency (Table 1). Among combretathiophenes, compounds **6**, **8**, **24**, **30**, and **31** were able to reduce viability/cell growth by at least 70% as measured by the MTT colorimetric method. On the

Scheme 3. Synthesis of Combretafurans 36 and 38



Scheme 4. Synthesis of the Cyclopentene Analogue of CA-4 40



other hand, all combretafurans, independent of the ring orientation, appeared efficacious at this concentration (33, 34, 36, 38). Similarly, the cyclopentene analogue of combretastatin was also efficacious (40).

We then performed full concentration–response curves of the compounds selected (see Supporting Information). In this set of experiments, CA-4 displayed an apparent IC_{50} of 2.3 ± 1.0 nM. Concentration–response curves supported the initial data on cytotoxicity, but most compounds had IC_{50} s in the high nanomolar range. The most potent combretathiofuran compound was 31, with an IC_{50} of 79 ± 67 nM. Although compounds 6 and 8 were not remarkably potent (IC_{50} over 300 nM), their activity is of interest because the moieties present on ring B display some degree of novelty. To confirm their potential activity on tubulin, we then performed FACS analysis to investigate their effect on the cell cycle (Figure 3). Both of these compounds were able to induce a G2/M block which might be indicative of their antitubulin activity. Combretafurans and the cyclopentane analogue were, on the other hand, rather potent. The most potent compound was represented by 34, which displayed an IC_{50} of approximately 2.4 ± 1.3 nM.

Analysis of the most potent compounds revealed that 31, 34, 38, and 40 all bear the 4-methoxy-3-hydroxy substitution. Indeed, this is the archetypical ring substitution that has been shown by many as being the most efficacious.⁵

We then proceeded to confirm the mechanism of action of these drugs. As these drugs displayed similar cytotoxicity in HeLa cells (Table 1), we then proceeded with this characterization in this latter cell line. First, we performed FACS analysis. From previous experiences, cells are grown for 16 h in the presence of 3 times the IC_{50} concentration and the DNA content is monitored with propidium iodide. All compounds were able to induce a severe G2/M block, which eventually leads to cell death (Figure 4).

Last, we directly investigated tubulin polymerization, visually (Figure 5a), on Western blots (Figure 5b) and via a tubulin polymerization *in vitro* assay. When cells were treated for 16 h with 3 times the IC_{50} concentration, the tubulin cytoskeleton (recognized with a specific antibody), clearly observable in control cells, disappeared in all treated samples.

To confirm this finding, cells were grown in the presence of 1, 31, 34, 38, or 40 and proteins were extracted in the presence of paclitaxel, which prevents further tubulin rearrangements (Figure 5b). Western blotting of the pelletable fraction and the soluble fraction then allows distinction between the polymerized and free form of tubulin.¹⁵ Indeed, while in control cells tubulin was present in similar amounts in the polymerized (pellet) and free form (supernatant). The equilibrium was significantly shifted toward the free form when cells were treated with 1 or with any of the compounds characterized. This is yet further evidence that inhibition of tubulin polymerization represents the primary mechanism of action of these compounds.

Last, we performed an *in vitro* tubulin polymerization assay. Compound 1 displayed an IC_{50} of 1.2 ± 0.05 . Compound 31 displayed an IC_{50} of 3.5 ± 0.2 . Compound 38 displayed an IC_{50} of 2.2 ± 1.0 , and compound 40 displayed an IC_{50} of 1.5 ± 0.1 . Compounds 1, 31, and 40 inhibited tubulin polymerization fully, while compound 38 inhibited about 50% of tubulin polymerization. The latter data might in part explain the different cell cycle pattern (Figure 4) elicited by this molecule.

IN VITRO METABOLISM

Human liver microsomes and the S9 system, which contains both liver cytosol and microsomes, were used to assess the *in vitro* metabolic stability of compounds 31, 38, and 40 in comparison to CA-4. In particular, phase I metabolism was

Table 1. Cytotoxicity in SH-SY5Y and HeLa Cells of the Synthesized Compounds^a

compd	SHSY-5Y		HeLa IC ₅₀ , nM
	viability (1 μ M), %	IC ₅₀ , nM	
1	23 \pm 2	2.3 \pm 1.0	1.7 \pm 4.1
6	27 \pm 4	350 \pm 70	420 \pm 67
7	80 \pm 2		
8	30 \pm 1	310 \pm 46	420 \pm 21
9	94 \pm 8		
10	52 \pm 3		
11	97 \pm 4		
12	93 \pm 8		
13	84 \pm 7		
14	100 \pm 16		
15	108 \pm 11		
16	45 \pm 3		
17	91 \pm 5		
18	91 \pm 3		
19	49 \pm 3		
20	83 \pm 2		
21	90 \pm 4		
22	90 \pm 5		
23	91 \pm 5		
24	28 \pm 1	330 \pm 120	430 \pm 17
25	82 \pm 14		
26	65 \pm 9		
27	93 \pm 6		
28	51 \pm 3		
29	109 \pm 8		
30	31 \pm 1	480 \pm 107	420 \pm 34
31	29 \pm 3	79 \pm 67	200 \pm 79
33	23 \pm 1	28 \pm 1.0	17 \pm 5.2
34	23 \pm 1	2.4 \pm 1.3	3.1 \pm 0.8
36	24 \pm 1	34 \pm 12	170 \pm 55
38	20 \pm 2	9.4 \pm 1.7	20.0 \pm 11.5
40	33 \pm 6	37 \pm 20	300 \pm 180

^a Values in the second column represent % of viable cells after 48 h of treatment with 1 μ M compound. Values in the last column represent the calculated IC₅₀ values for those compounds in which a full concentration response curve was performed. Values are the mean \pm SD of 12 determinations from 3 separate experiments. IC₅₀ values were determined only for the most potent compounds.

performed in microsomal incubations in the presence of a NADP(H)-regenerating system, allowing evaluation of the metabolites arising from oxidative metabolic pathways. Phase II metabolism was investigated in microsomes and S9 fractions by using the appropriate cofactor to evaluate the glucuronide and sulfate conjugates formation. Moreover, microsomal incubations were also carried out in the presence of the nucleophilic trapping agent GSH capable of reacting with electrophilic intermediate species. Indeed, the formation of reactive intermediates in the metabolism represents a potential liability in drug discovery and development potentially leading to adverse reactions and/or toxicity via covalent binding to cellular proteins and enzymes.¹⁶ First, the *Z*–*E* isomerization of the olefin bond and the formation

of quinone species were observed in the metabolic fate of CA-4, while this obviously did not occur for the rigidified analogues.

The in vitro human hepatic microsomal metabolism of CA-4 involves three main metabolic pathways: O-demethylation, aromatic hydroxylation, and glucuronidation.⁷ Compounds **31**, **38**, and **40** shared a similar metabolic pattern. Indeed, as reported in the Table 2, the metabolites arising from O-demethylation, aromatic hydroxylation, and conjugation were observed in LC–MS² chromatograms (see Supporting Information). Similarly the formation of quinonic species was also established through the identification of their GSH adducts. Indeed GSH adducts can be easily detected by LC–MS using full-scan and product ion scan modes (see Supporting Information). However, compound **31** also showed an additional metabolic activation pathway, possibly arising from the oxidation of thiophene ring. Again, the presence in the LC–MS² traces (*m/z* = 696, Supporting Information) of another series of GSH adducts, generated by both S-oxidation or epoxidation on ring C, could be considered diagnostic. In contrast, compounds **38** and **40** did not show any additional metabolic activation on ring C. All compounds tested in the phase I microsomal incubations showed an extent of transformation that did not exceed 5% in the first hour of incubation. As previously reported for CA-4, the glucuronidation pathway was prominent. This was the case also for compounds **31**, **38**, and **40**. Yet from a quantitative viewpoint, the glucuronidation was slower for **38** and **40** compared to CA-4.

MOLECULAR MODELING

Molecular modeling studies were performed to investigate the potential binding ability of these compounds to the colchicine binding site of α , β -tubulin. Docking studies showed that **34**, the most active compound, occupies the colchicine binding site of tubulin in agreement with the X-ray structure complex of DAMA–colchicine–tubulin.¹⁷ The trimethoxyphenyl moiety in ring A of **34** was positioned in the binding cavity buried in the β -subunit. The thiol group of β C241 formed a hydrogen bond with the oxygen atom of one of the methoxy groups, and several amino acids of β -tubulin formed hydrophobic interactions with the trimethoxyphenyl moiety of **34**. The hydroxyl group of ring B formed a hydrogen bond with the main chain nitrogen atom of α V181 (Figure 6). Also in the case of compounds **31**, **38**, and **40** the docked pose is similar to the colchicine binding mode. The missing hydrogen bonding interaction with α V181 possibly explains the reduced biological activity of compounds **30**, **33**, and **36** (see Supporting Information).

CONCLUSIONS

The present manuscript describes the use of a two-step regioselective Suzuki to generate potent rigid analogues of combretastatin. As a proof of principle, three different scaffolds were prepared. All scaffolds prepared were novel, and therefore, direct comparisons with alternative synthetic strategies are not possible. Nonetheless, literature/patent data can be used to support the easiness of this strategy.^{9,18} For example, we have previously synthesized 3,4-diphenyl substituted furan compounds,⁹ which can therefore be directly compared to the 2,3-diphenyl substituted furans described here. The furan with the 3,4,5-trimethoxyphenyl ring A and the 4-methoxy-3-hydroxyphenyl ring B was prepared in five synthetic steps using a complicated intramolecular aldol condensation as a key step.

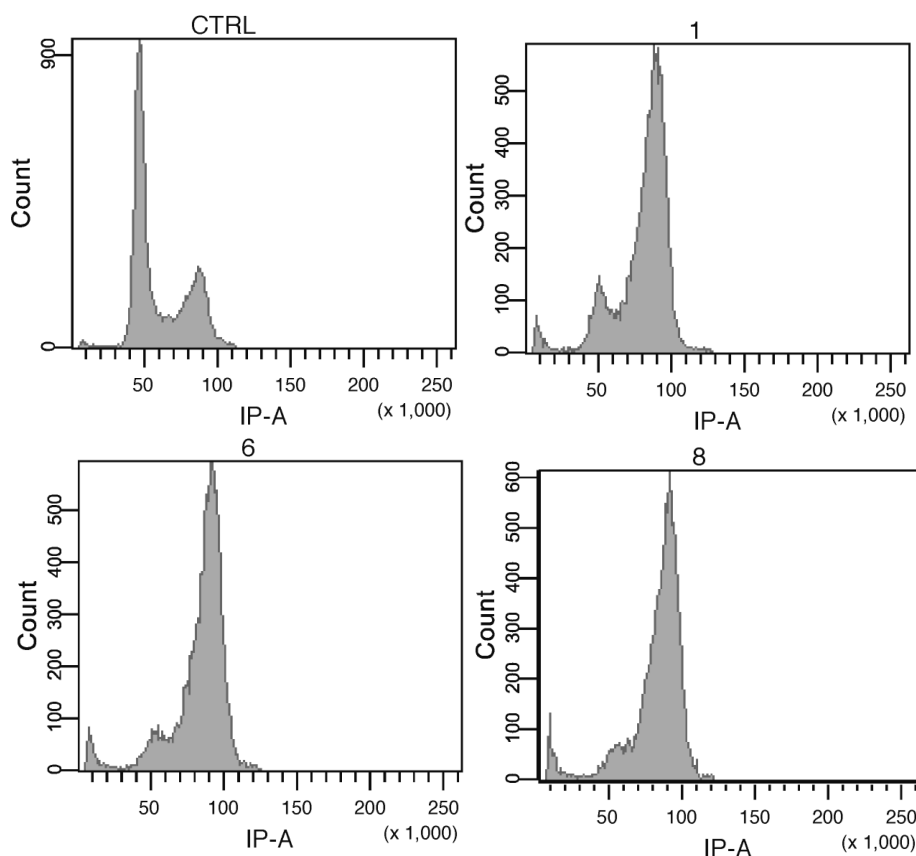


Figure 3. Analogues bearing atypical substitutions on ring A induce cell cycle arrest. Cell cycle analysis of HeLa cells treated for 16 h with vehicle (ctrl) or $3 \times \text{IC}_{50}$ values of indicated compounds. Data are representative of three separate experiments. Similar results were obtained in separate experiments when drugs were incubated for 8 or 24 h. The Y-axis represents cell number, and the X-axis represents fluorescence on a linear scale.

CA-4 has already entered clinical trials. Possible improvements over this molecule might be metabolic stability, the absence of cis–trans double bond isomerization (which might lead to off-target effects), and a longer half-life. It could therefore be envisaged that analogues that retain the potency and efficacy of CA-4 but that are different in the pharmacokinetic profile might be useful. Indeed, it should also be considered that drug interactions are becoming a sensible issue in cancer therapy,²⁰ and therefore, having more than one option could be desirable in the different therapeutic schemes. In this respect, the synthetic strategy described here might be helpful and the improved pharmacokinetic stability of two of the five-membered rings described (38 and 40) might be perceived as an improvement. As tubulin isoforms are different in different tumor types,²¹ it could also be envisaged that this strategy could be employed to generate a battery of novel analogues (bearing a five-membered ring or any other kind) with increased selectivity. Nonetheless, a number of rigidified analogues have already been synthesized, and therefore, it is time to seek such differences.

EXPERIMENTAL SECTION

Chemistry. Commercially available reagents and solvents were used without further purification. Dimethylformamide (DMF) was purified by distillation at reduced pressure, collecting the fraction having bp 76 °C at 39 mmHg and storing on activated molecular sieves (4 Å). When needed, the reactions were performed in flame- or oven-dried glassware under a positive pressure of dry N₂ or in a Schlenk tube.

Melting points were determined in open glass capillary with a Stuart scientific SMP3 apparatus and are uncorrected. All the compounds were checked by IR (FT-IR THERMO-NICOLET AVATAR), ¹H and ¹³C APT (JEOL ECP 300 MHz), and mass spectrometry (Thermo Finnigan LCQ-deca XP-plus) equipped with an ESI source and an ion trap detector. Chemical shifts are reported in parts per million (ppm). Column chromatography was performed on silica gel Merck Kieselgel 70–230 mesh ASTM or silica gel Merck Kieselgel 230–400 ASTM when using Biotage Isolera. Thin layer chromatography (TLC) was carried out on 5 cm × 20 cm plates with a layer thickness of 0.25 mm (Merck silica gel 60 F₂₅₄). When necessary, they were developed with KMnO₄. The purity of the target compounds (>95%) was analyzed via elemental analysis and was within ±0.4% of the calculated value. All molecular modeling calculations were performed using the software Autodock 4¹⁹ running on a Tesla workstation equipped with two Intel Xenon X5650, 2.67 GHz.

The geometry of the colchicine was taken from the structure of the tubulin filed in the Brookhaven Protein Data Bank (entry code 1SA0).¹⁶ For the docking a grid spacing of 0.375 Å and 56 × 60 × 50 number of points were used. The grid was centered on the mass center of the colchicine coordinates. The GA-LS method was adopted using the default settings. Charges were assigned to the protein using the program ADT (AutoDock Tools). Autodock generated 100 possible binding conformations for ligands. To validate the use of the Autodock program, the docking studies were performed on the reference compounds colchicine and combretastatin A-4. Autodock successfully reproduced the binding conformations reported in the literature with acceptable root-mean-square deviation (rmsd < 1 Å) of atom coordinates.

3-Bromo-4-(3,4,5-trimethoxyphenyl)thiophene (5). To a solution of commercially available 3,4-dibromothiophene (1.92 g, 7.97 mmol)

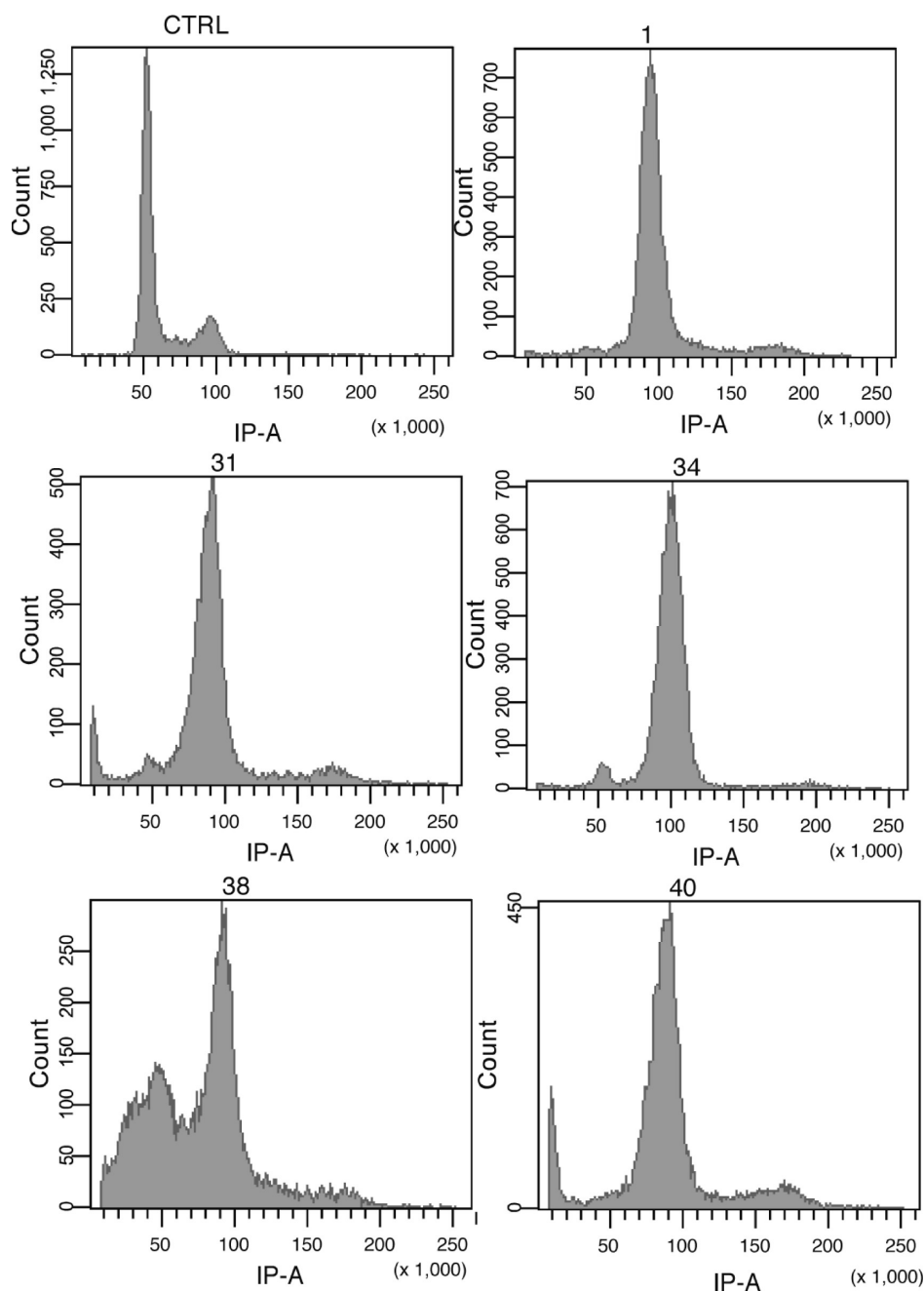


Figure 4. Combretastatin and the most potent analogues synthesized induce cell cycle arrest. Cell cycle analysis of HeLa cells treated for 16 h with vehicle (ctrl) or $3 \times \text{IC}_{50}$ values of indicated compounds. Data are representative of three separate experiments. Similar results were obtained in separate experiments when drugs were incubated for 8 or 24 h. The Y-axis represents cell number, and the X-axis represents fluorescence on a linear scale.

and 3,4,5-trimethoxybenzene boronic acid (0.56 g, 2.66 mmol) in 43 mL of DMF, the tetrakis(triphenylphosphine)palladium (0.15 g, 0.13 mmol) and an aqueous solution of sodium carbonate monohydrate (0.99 g, 7.97 mmol) were added, and the mixture was stirred. The mixture was then warmed at 50 °C for 4.5 h. The mixture was diluted with water and extracted with ethyl acetate ($\times 3$). The combined organic fractions were washed with brine ($\times 1$), dried over sodium sulfate, and concentrated under vacuum. The crude product was purified by flash column chromatography by using petroleum ether/ethyl acetate (8:2) as eluent to give 0.52 g of **5** as a white solid (59%).

General Procedure for the Synthesis of Thiophenes (6–31). The 3-bromo-4-(3,4,5-trimethoxyphenyl)thiophene (**5**) (1.2 equiv) was

dissolved in DMF, and 1 equiv of the corresponding boronic acid (A6-31) was added. The tetrakis(triphenylphosphine)palladium (0.05 equiv) and an aqueous solution of sodium carbonate monohydrate (3 equiv) were added and stirred. The mixture was then heated at 80 °C until the reaction was finished. The mixture was diluted with water and extracted with ethyl acetate ($\times 3$). The combined organic fractions were washed with brine ($\times 1$) and dried over anhydrous sodium sulfate and concentrated in vacuo. The crude product was purified by column chromatography.

3-Bromo-2-(3,4,5-trimethoxyphenyl)furan (32). To a solution of commercially available 2,3-dibromofuran (1 g, 4.42 mmol) and 3,4,5-trimethoxybenzene boronic acid (0.39 g, 1.84 mmol) in

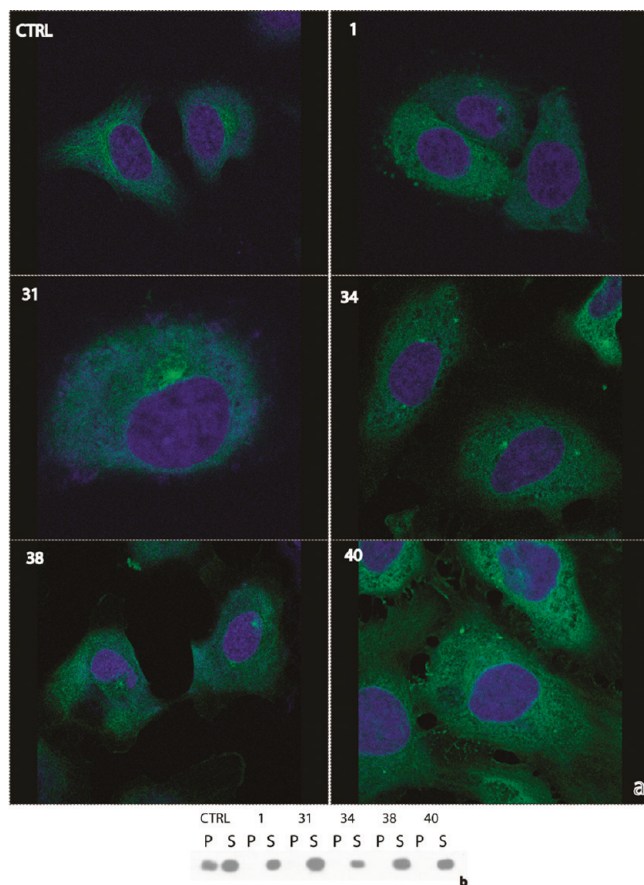


Figure 5. Combretastatin and the most potent compounds synthesized affect tubulin polymerization. (a) Immunofluorescence using an anti- α -tubulin antibody (green) and DRAQS (blue) for nuclear staining of control cells (ctrl) or cells treated for 24 h with $3 \times \text{IC}_{50}$ value of the indicated compounds. Images have been obtained with a $63\times$ oil immersion objective. (b) Western blot of α -tubulin extracted in the presence of paclitaxel from Hela cells treated with the indicated compounds at $3 \times \text{IC}_{50}$ value. Results are representative of three separate experiments. P = pelletable fraction. S = soluble fraction.

Table 2. Metabolic Profile for CA-4, 31, 38, and 40

metabolic pathway	CA-4	31	38	40
O-demethylation	+	+	+	+
aromatic hydroxylation (ring B)	+	+	+	+
metabolic activation				
quinones	+	+	+	+
ring C	–	+	–	–
phase I transformation (%) ^a	≤ 5	≤ 5	≤ 5	≤ 5
conjugation				
glucuronides	+	+	+	+
sulfates	+	+	+	+
phase II transformation (%) ^a	~ 40	~ 40	~ 20	~ 30

^aExpressed as peak area percent obtained from LC–UV analyses of incubation extracts ($t = 60$ min).

10 mL of DMF, the tetrakis(triphenylphosphine)palladium (0.11 g, 0.09 mmol) and an aqueous solution of sodium carbonate monohydrate (0.68 g 5.51 mmol) were added, and the mixture was stirred. The mixture was then warmed at 50°C for 5 h. The mixture was diluted with water and extracted with ethyl acetate ($\times 3$). The combined organic fractions were washed with brine ($\times 1$), dried over sodium

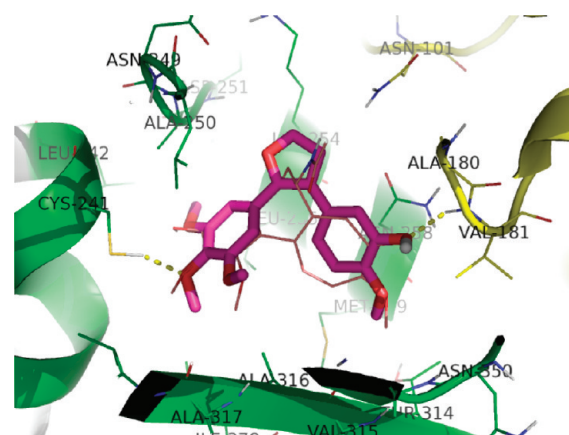


Figure 6. Superimposition of the presumptive conformation of active 34 (stick model) on top of the X-ray structure of DAMA–colchicine (wire model). The structures are docked into the colchicine binding site of tubulin (PDB entry 1SA0). The backbone of tubulin is shown as ribbon representation (α -tubulin, yellow; β -tubulin, blue). The amino acids of tubulin within 4.0 \AA from colchicine are shown as wire models. Hydrogen bonds (distance of $<3 \text{ \AA}$) are shown as dotted lines.

sulfate, and concentrated under vacuum. The crude product was purified by flash column chromatography by using petroleum ether/ethyl acetate (8:2) as eluent to give 0.38 g of a white solid (66%).

3-(4-Methoxyphenyl)-2-(3,4,5-trimethoxyphenyl)furan (33). The previously synthesized 3-bromo-2-(3,4,5-trimethoxyphenyl)furan (33) (100 mg, 0.32 mmol) was dissolved in DMF (2.5 mL) and stirred. The commercially available 4-methoxybenzene boronic acid (40 mg, 0.27 mmol), tetrakis(triphenylphosphine)palladium (15 mg, 0.013 mmol), and an aqueous solution of sodium carbonate monohydrate (99 mg, 0.80 mmol) were added, and the mixture was stirred. The mixture was then heated at 70°C for 3 h. The mixture was diluted with water and extracted with ethyl acetate ($\times 3$). The combined organic fractions were washed with brine ($\times 1$), dried over sodium sulfate, and concentrated under vacuum. The crude product was purified by flash column chromatography by using petroleum ether/ethyl acetate (8:2) as eluent to give 53 mg of a light yellow oil (59%).

2-Methoxy-5-[2-(3,4,5-trimethoxyphenyl)-3-furyl]phenol (34). To a solution of the previously synthesized 3-bromo-2-(3,4,5-trimethoxyphenyl)furan (32), 60 mg, 0.19 mmol and (3-hydroxy-4-methoxyphenyl)boronic acid (29 mg, 0.16 mmol) in 2.5 mL of DMF, the tetrakis(triphenylphosphine) palladium (9 mg, 0.01 mmol) and an aqueous solution of sodium carbonate monohydrate (59 mg 0.80 mmol) were added, and the mixture was stirred. The mixture was then heated at 70°C for 2 h. The mixture was diluted with water and extracted with ethyl acetate ($\times 3$). The combined organic fractions were washed with brine ($\times 1$) and dried over sodium sulfate and concentrated under vacuum. The crude product was purified by flash column chromatography by using petroleum ether/ethyl acetate (8:2) as eluent to give 31 mg of an amorphous yellow solid (54%).

3-Bromo-2-(4-methoxyphenyl)furan (35). To a solution of commercially available 2,3-dibromofuran (0.8 g, 3.54 mmol) and 4-methoxybenzene boronic acid (0.224 g, 1.48 mmol) in 8 mL of DMF, the tetrakis(triphenylphosphine)palladium (0.085 g, 0.07 mmol) and an aqueous solution of sodium carbonate monohydrate (0.55 g, 4.43 mmol) were added, and the mixture was stirred. The mixture was then warmed at 50°C for 3 h. The mixture was diluted with water and extracted with ethyl acetate ($\times 3$). The combined organic fractions were washed with brine ($\times 1$) and dried over sodium sulfate and concentrated under vacuum. The crude product was purified by flash column chromatography by using petroleum ether/ethyl acetate (9:1) as eluent to give 0.24 g of a yellow oil (65%).

2-(4-Methoxyphenyl)-3-(3,4,5-trimethoxyphenyl)furan (36). The previously synthesized 3-bromo-2-(4-methoxyphenyl)furan (35) (100 mg, 0.40 mmol) was dissolved in DMF (2.5 mL), and the mixture was stirred. The commercially available 3,4,5-trimethoxybenzene boronic acid (70 mg, 0.33 mmol), tetrakis(triphenylphosphine)palladium (19 mg, 0.016 mmol), and an aqueous solution of sodium carbonate monohydrate (123 mg, 0.99 mmol) were added, and the mixture was stirred. The mixture was then heated at 70 °C for 3 h. The mixture was diluted with water and extracted with ethyl acetate ($\times 3$). The combined organic fractions were washed with brine ($\times 1$) and dried over sodium sulfate and concentrated under vacuum. The crude product was purified by flash column chromatography by using petroleum ether/ethyl acetate (8:2) as eluent to give 54.1 mg of an amorphous yellow solid (48%).

5-(3-Bromo-2-furyl)-2-methoxyphenol (37). To a solution of the commercially available 2,3-dibromofuran (1.1 g, 4.43 mmol) and (3-hydroxy-4-methoxyphenyl)boronic acid (0.33 g, 1.84 mmol) in 10 mL of DMF, the tetrakis(triphenylphosphine)palladium (0.11 g, 0.09 mmol) and an aqueous solution of sodium carbonate monohydrate (0.69 g, 5.53 mmol) were added, and the mixture was stirred. The mixture was then warmed at 50 °C for 5 h. The mixture was diluted with water and extracted with ethyl acetate ($\times 3$). The combined organic fractions were washed with brine ($\times 1$) and dried over sodium sulfate and concentrated under vacuum. The crude product was purified by flash column chromatography by using petroleum ether/ethyl acetate (8:2) as eluent to give 0.42 g of an amorphous reddish solid (84%).

2-Methoxy-5-[3-(3,4,5-trimethoxyphenyl)-2-furyl]phenol (38). To a solution of the previously synthesized 5-(3-bromo-2-furyl)-2-methoxyphenol (37) (110 mg, 0.41 mmol) and the commercially available 3,4,5-trimethoxybenzene boronic acid (72 mg, 0.34 mmol) in 2.5 mL of DMF, tetrakis(triphenylphosphine)palladium (20 mg, 0.02 mmol) and an aqueous solution of sodium carbonate monohydrate (127 mg, 1.02 mmol) were added, and the mixture was stirred. The mixture was then heated at 70 °C for 2 h. The mixture was diluted with water and extracted with ethyl acetate ($\times 3$). The combined organic fractions were washed with brine ($\times 1$) and dried over sodium sulfate and concentrated under vacuum. The crude product was purified by flash column chromatography by using petroleum ether/ethyl acetate (8:2) as eluent to give 0.08 g of an amorphous yellow solid (66%).

5-(2-Bromocyclopent-1-en-1-yl)-1,2,3-trimethoxybenzene (39). To a solution of the commercially available 1,2-dibromocyclopentene (0.73 g, 3.22 mmol) and 3,4,5-trimethoxybenzene boronic acid (0.20 g, 0.92 mmol) in 10 mL of DMF, tetrakis(triphenylphosphine)palladium (0.05 g, 0.05 mmol) and an aqueous solution of sodium carbonate monohydrate (0.34 g, 2.76 mmol) were added, and the mixture was stirred. The mixture was then warmed at 50 °C for 2 h. The mixture was diluted with water and extracted with ethyl acetate ($\times 3$). The combined organic fractions were washed with brine ($\times 1$) and dried over sodium sulfate and concentrated under vacuum. The crude product was purified by flash column chromatography by using petroleum ether/ethyl acetate (8:2) as eluent to give 0.07 g of a yellow oil (23%).

2-Methoxy-5-[2-(3,4,5-trimethoxyphenyl)cyclopent-1-en-1-yl]phenol (40). To a solution of the previously synthesized 5-(2-bromocyclopent-1-en-1-yl)-1,2,3-trimethoxybenzene (39) (60 mg, 0.19 mmol) and (3-hydroxy-4-methoxyphenyl)boronic acid (27 mg, 0.16 mmol) in 2.5 mL of DMF, tetrakis(triphenylphosphine)palladium (9 mg, 0.008 mmol) and an aqueous solution of sodium carbonate monohydrate (59 mg, 0.48 mmol) were added, and the mixture was stirred. The mixture was then heated at 70 °C for 1 h. The mixture was diluted with water and extracted with ethyl acetate ($\times 3$). The combined organic fractions were washed with brine ($\times 1$) and dried over sodium sulfate and concentrated under vacuum. The crude product was purified by flash column chromatography by using petroleum ether/ethyl acetate (8:2) as eluent to give 0.014 g of a white solid (44%).

Cell Culture and Cytotoxicity Assay. The SH-SY5Y human neuroblastoma cell line was obtained from ATCC (LGC Promochem Teddington, U.K.) and cultured in 50% DMEM and 50% F-12 supplemented with 10% fetal bovine serum, 2 mM L-glutamine, penicillin (100 $\mu\text{g}/\text{mL}$), and streptomycin (100 $\mu\text{g}/\text{mL}$). For cytotoxicity assays, cells were plated on 24-well plates and grown for 48 h in the presence or absence of combretastatin A-4 or the synthesized compounds. On the experimental day, cells were washed twice in Locke's solution (134 mM NaCl, 5 mM KCl, 4 mM NaHCO_3 , 10 mM HEPES [pH 7.6], 2.3 mM CaCl_2 , 1 mM MgCl_2 , 5 mM sucrose) and incubated for 30 min with MTT (250 $\mu\text{g}/\text{mL}$ in Locke's solution) at 37 °C. Reactions were then stopped and the crystals solubilized in isopropyl alcohol/HCl before being read at 570 nm in a spectrophotometer. To determine IC_{50} values, data were plotted and fitted using the Kaleidagraph software (Synergy Software, Reading, PA).

Immunocytochemistry. SH-SY5Y were plated on glass coverslips and grown to subconfluency in the presence or absence of drugs for 24 h. Coverslips were then fixed in paraformaldehyde (3.7%) for 20 min at room temperature. Cells were then washed once in phosphate buffered saline (PBS) and permeabilized in ice cold 80% MeOH for 10 min in ice. Cells were then washed twice in PBS and blocked with 0.2% cold fish gelatine. Anti- α -tubulin (mouse) primary antibody (Sigma-Aldrich, 1:1000) was incubated for 20 min at room temperature, and after three further washes, coverslips were incubated with a goat anti-mouse Alexa Fluor 488 (Molecular Probes, 1:2000) and Draq 5 (Cell Signaling 1:1000). Slides were then visualized in a Leica SP2 confocal microscopy.

In Vivo and in Vitro Tubulin Polymerization Assay. To measure the degree of tubulin polymerization in vivo, we used an adaptation of the methods described by Minotti et al.¹⁵ In brief, cells were grown in 75 cm^2 flasks in the presence or absence of drugs ($3 \times \text{IC}_{50}$) for 16 h. Cells were then trypsinized and centrifuged at 600g for 3 min and washed once by PBS. Cells were then resuspended in 70 μL of hypotonic buffer (20 mM Tris-HCl, pH 6.8, 1 mM MgCl_2 , 2 mM EGTA, protease inhibitors, 0.5% NP-40) containing 4 $\mu\text{g}/\text{mL}$ paclitaxel. Lysates were incubated for 10 min at room temperature. Lysates were then corrected for protein amounts (Bradford assay, Sigma-Aldrich), and 50 μg (corresponding to 50 μL) was centrifuged at 13 000 rpm for 15 min at room temperature. Supernatant and pellet were then resuspended in equal volumes of SDS loading buffer and run on a 10% SDS-polyacrylamide gel. After transfer of proteins to nitrocellulose (blocked in 5% milk), tubulin was identified with an anti- α -tubulin primary antibody (1:1000, Sigma-Aldrich) and anti-mouse secondary antibody peroxidase-conjugated (1:8000, Amersham Bioscience) and visualized by chemiluminescence (Supersignal WestPico, Pierce). In vitro polymerization was performed using a commercially available kit (Cytoskeleton Inc.).

Flow-Cytometric Analysis of Cell-Cycle Status. SH-SY5Y cells grown in the presence or absence of compounds for 16 h were washed once in PBS and resuspended in 1 mL of 30:70 ice cold PBS/EtOH and stored at -20 °C. Cells were then washed twice in PBS and resuspended in PBS containing RNase (100 $\mu\text{g}/\text{mL}$) for 30 min at room temperature. DNA was then stained with a PBS solution containing 5 mM EDTA and 100 $\mu\text{g}/\text{mL}$ propidium iodide for 30 min at room temperature in the dark. Cell cycle analysis was determined with a FACSVantage SE DiVa (Becton Dickinson).

In Vitro Metabolism and Modeling. The procedure to investigate in vitro metabolism and the modeling protocol are detailed in the Supporting Information.

■ ASSOCIATED CONTENT

Supporting Information. Characterization of all compounds synthesized (mp, IR, MS, and ^1H and ^{13}C NMR data), elemental analysis results of all target compounds, molecular modeling binding modes of 30, 31, 33, 36, 38, and 40, and

metabolism procedures and results for **1**, **31**, **38**, and **40**. This material is available free of charge via the Internet at <http://pubs.acs.org>.

AUTHOR INFORMATION

Corresponding Author

*Phone: +39-0321-375857. Fax: +39-0321-375821. E-mail: tron@pharm.unipmn.it

Author Contributions

[†]These authors equally contributed to the present work.

ACKNOWLEDGMENT

Financial support from M.I.U.R. PRIN 2008 Italy and Associazione per la Ricerca sul Cancro (AIRC) Italy are gratefully acknowledged. S.T. thanks Italian Ministry of Foreign Affairs for the Ph.D. fellowship.

ABBREVIATIONS USED

CA-4, combretastatin A-4; CA-4P, combretastatin A-4 phosphate; MTT, 3-(4,5-dimethylthiazol-2-yl)-2,5-diphenyltetrazolium bromide; GSH, glutathione reduced

REFERENCES

- (1) Pettit, G. R.; Singh, S. B.; Hamel, E.; Lin, C. M.; Alberts, D. S.; et al. Isolation and structure of the strong cell growth and tubulin inhibitor combretastatin A-4. *Experientia* **1989**, *45*, 209–211.
- (2) (a) Bibby, M. C. Combretastatin anticancer drugs. *Drugs Future* **2002**, *27*, 475–480. (b) Pinney, K. G.; Jelinek, C.; Edvardsen, K.; Chaplin, D. J.; Pettit, G. R. The Discovery and Development of the Combretastatins. In *Antitumor Agents from Natural Products*; Kingston, D., Newman, D., Cragg, G., Eds.; CRC Press: Boca Raton, FL, 2005; pp 23–46.
- (3) (a) Kanthou, C.; Tozer, G. M. The tumor vascular targeting agent combretastatin A-4 phosphate induces reorganization of the actin cytoskeleton and early membrane blebbing in human endothelial cells. *Blood* **2002**, *99*, 2060–2069. (b) Chaplin, D. J.; Hill, S. A. The development of combretastatin A-4 phosphate as a vascular targeting agent. *Int. J. Radiat. Oncol. Biol. Phys.* **2002**, *54*, 1491–1496. (c) West, C. M. L.; Price, P. Combretastatin A4 phosphate. *Anti-Cancer Drugs* **2004**, *15*, 179–186. (d) Siemann, D. W.; Chaplin, D. J.; Walicke, P. A. A review and update of the current status of the vasculature-disabling agent combretastatin-A4 phosphate (CA4P). *Expert Opin. Invest. Drugs* **2009**, *18*, 189–197.
- (4) Delmonte, A.; Sessa, C. AVE8062: a new combretastatin derivative vascular disrupting agent. *Expert Opin. Invest. Drugs* **2009**, *18*, 1541–1548.
- (5) Tron, G. C.; Pirali, T.; Sorba, G.; Pagliai, F.; Busacca, S.; Genazzani, A. A. Medicinal chemistry of combretastatin A4: present and future directions. *J. Med. Chem.* **2006**, *49*, 3033–3044.
- (6) (a) Gaukroger, K.; Hadfield, J. A.; Lawrence, N. J.; Nlan, S.; McGown, A. T. Structural requirements for the interaction of combretastatins with tubulin: How important is the trimethoxy unit? *Org. Biomol. Chem.* **2003**, *1*, 3033–3037. (b) Beale, T. M.; Myers, R. M.; Shearman, J. W.; Charnock-Jones, D. S.; Brenton, J. D.; Gergely, F. V.; Ley, S. V. *Med. Chem. Commun.* **2010**, *1*, 202–208.
- (7) Aprile, S.; Del Grosso, E.; Tron, G. C.; Grosa, G. In vitro metabolism study of combretastatin A-4 in rat and human liver microsomes. *Drug Metab. Dispos.* **2007**, *35*, 2252–2261.
- (8) (a) Nam, N.-H. Combretastatin A-4 analogues as antimitotic antitumor agents. *Curr. Med. Chem.* **2003**, *10*, 1697–1722. (b) Hsieh, H. P.; Liou, J. P.; Mahindroo, N. *Curr. Pharm. Des.* **2005**, *11*, 1655–1677. Chaudari, A.; Pandeya, S. N.; Kumar, P.; Sharma, P. P.; Gupta, S.; Soni, N.; Verma, K. K.; Bhardwaj, G. Combretastatin A-4 analogues as anticancer agents. *Mini-Rev. Med. Chem.* **2007**, *12*, 1186–1205.

- (9) Pirali, T.; Busacca, S.; Beltrami, L.; Imovilli, D.; Pagliai, F.; Miglio, G.; Massarotti, A.; Verotta, L.; Tron, G. C.; Sorba, G.; Genazzani, A. A. Synthesis and cytotoxic evaluation of combretafurans, potential scaffolds for dual-action antitumoral agents. *J. Med. Chem.* **2006**, *49*, 5372–5376.

- (10) (a) Cafici, L.; Pirali, T.; Condorelli, F.; Del Grosso, E.; Massarotti, A.; Sorba, G.; Canonico, P. L.; Tron, G. C.; Genazzani, A. A. Solution-phase parallel synthesis and biological evaluation of combretatriazoles. *J. Comb. Chem.* **2008**, *10*, 732–740. (b) Romagnoli, R.; Baraldi, P. G.; Cruz-Lopez, O.; Lopez Cara, C.; Carrion, M. D.; Brancale, A.; Hamel, E.; Chen, L.; Bortolozzi, R.; Basso, G.; Viola, G. Synthesis and antitumor activity of 1,5-disubstituted 1,2,4-triazoles as cis-restricted combretastatin analogues. *J. Med. Chem.* **2010**, *53*, 4248–4258. Wang, L.; Woods, K. W.; Li, Q.; Barr, K. J.; McCroskey, R. W.; Hannick, S. M.; Gherke, L.; Credo, R. B.; Hui, Y.-H.; Marsh, K.; Warner, R.; Lee, J. Y.; Zielinski-Mozng, N.; Frost, D.; Rosemberg, S. H.; Sharm, H. L. Potent orally active heterocycle-based combretastatin A-4 analogues: synthesis, structure–activity relationship, pharmacokinetics, and in vivo antitumor activity. *J. Med. Chem.* **2002**, *45*, 1697–1711. Ohsumi, K.; Hatanaka, T.; Fujita, K.; Nakagawa, R.; Fukuda, Y.; Nihei, Y.; Suga, Y.; Morinaga, Y.; Akiyama, Y.; Tsuji, T. *Bioorg. Med. Chem. Lett.* **1998**, *8*, 3153–3158.

- (11) (a) Cushman, M.; Nagarathnam, D.; Gopal, D.; He, H.-M.; Lin, C. M.; Hamel, E. *J. Med. Chem.* **1992**, *35*, 2293–2306. (b) Gaukroger, K.; Hadfield, J. A.; Hepworth, L. A.; Lawrence, N. J.; McGown, A. T. Novel synthesis of cis and trans isomers of combretastatin A-4. *J. Org. Chem.* **2001**, *66*, 8135–8138.

- (12) Handy, S. T.; Zhang, Y. A simple guide for predicting regioselectivity in the coupling of polyhaloheteroaromatics. *Chem. Commun.* **2006**, 299–301.

- (13) (a) Nguyen, T. L.; McGrath, C.; Hermone, A. R.; Burnett, J. C.; Zaharevitz, D. W.; Day, B. W.; Wipf, P.; Hamel, E.; Gussio, R. A common pharmacophore for a diverse set of colchicine site inhibitors using a structure-based approach. *J. Med. Chem.* **2005**, *48*, 6107–6116. (b) Kong, Y.; Grembecka, J.; Edler, M. C.; Hamel, E.; Mooberry, S.; Sabat, M.; Rieger, J.; Brown, M. L. Structure-based discovery of a boronic acid bioisostere of combretastatin A-4. *Chem. Biol.* **2005**, *12*, 1007–1014.

- (14) Tron, G. C.; Pagliai, F.; Del Grosso, E.; Genazzani, A. A.; Sorba, G. Synthesis and cytotoxic evaluation of combretafurazans. *J. Med. Chem.* **2005**, *48*, 3260–3268.

- (15) Minotti, A. M.; Barlow, S. B.; Cabral, F. Resistance to anti-mitotic drugs in Chinese hamster ovary cells correlates with changes in the level of polymerized tubulin. *J. Biol. Chem.* **1991**, *266*, 3987–3994.

- (16) Evans, D. C.; Watt, A. P.; Nicoll-Griffith, D. A.; Baillie, T. A. Drug–protein adducts: an industry perspective on minimizing the potential for drug bioactivation in drug discovery and development. *Chem. Res. Toxicol.* **2004**, *17*, 3–16.

- (17) Ravelli, R. B.; Gigant, B.; Curmi, P. A.; Jourdain, I.; Lachkar, S.; Sobel, A.; Knossow, M. Insight into tubulin regulation from a complex with colchicines and a stathmin-like domain. *Nature* **2004**, *428*, 198–202.

- (18) Zhang, W.; Yang, Q.; Wu, Y.; Wu, L.; Li, W.; Qiao, F.; Bao, K.; Zhang, L. Preparation of 2,3-Diarylthiophene Derivatives As Antitumor Agents. CN Patent 101429189, 2009. At least nine synthetic steps are required to prepare the thiophene analogues of combretastatin reported in this patent.

- (19) Morris, G. M.; Goodsell, D. S.; Halliday, R. S.; Huey, R.; Hart, W. E.; Belew, R. K.; Olson, A. Automated docking using a Lamarckian genetic algorithm and empirical binding free energy function. *J. Comput. Chem.* **1998**, *19*, 1639–1662.

- (20) Riechelmann, R. P.; Del Giglio, A. Drug interactions in oncology: how common are they? *Ann. Oncol.* **2009**, *12*, 1907–1912.

- (21) Leandro-Garcia, L. J.; Leskela, S.; Landa, I.; Montero-Conde, C.; Lopez-Jiménez, E.; Leton, R.; Cascon, A.; Robledo, M.; Rodriguez-Antona, C. Tumoral and tissue-specific expression of the major human β -tubulin isotypes. *Cytoskeleton* **2010**, *67*, 214–223.